

UDC 538.915

ELECTRONIC AND DYNAMICAL PROPERTIES OF BULK AND LAYERED MoS₂

A.V. KRIVOSHEEVA, V.L. SHAPOSHNIKOV, V.E. BORISENKO, J.-L. LAZZARI*

*Belarusian State University of Informatics and Radioelectronics
P. Browka 6, 220013 Minsk, Belarus***Centre Interdisciplinaire de Nanoscience de Marseille (CINaM), Campus de Luminy, Marseille, France**Submitted April, 7, 2014*

Electronic and dynamical properties of MoS₂ are determined by means of theoretical calculations. Various numbers of layers with different thickness of the vacuum layer were considered. We have found that the band gap of bulk MoS₂ is increasing upon decreasing of the number of layers from 0.76 eV up to 1.85 eV, and transforms from indirect to direct one in one-monolayer structure. The influence of vacancies on the electronic properties of MoS₂ is analyzed and its dynamical properties are presented.

Key words: molybdenum disulfide, nanostructure, electronic properties, phonons.

Introduction

Last years new materials like graphene [1] or silicene [2-4] attract special attention due to possibilities of using in nanophotonics [1]. However, while graphene demonstrate preferably metallic behavior, the efforts are concentrated on the search for other 2D materials. The crystal lattice of molybdenum disulfide MoS₂ is similar to the one of graphene, as it has hexagonal structure and consists of alternating S-Mo-S layers attached to each other through Van der Waals forces. Such layers may be used in field-effect transistors, photovoltaic or photocatalytic devices [5, 6]. This material was reported to be semiconductor with an indirect band gap of 1.29 eV [7], whereas the single layer of MoS₂ was described as direct-gap semiconductor with a band gap of 1.8 eV [8]. It was shown that the band gaps in bilayer MoS₂, like in bilayer graphene, could be tuned by external electric fields [9]. Splendiani *et al.* [10] observed a surprising emergence of photoluminescence in MoS₂ layers. This observation was consistent with the theoretical prediction of indirect to direct band-gap transition in going from multilayer to monolayer MoS₂. The latter was predicted to be a direct gap semiconductor ($E_g = 1.72$ eV) [11], while bilayer MoS₂ was found to be an indirect gap compound ($E_g = 1.52$ eV) and the energy band gap of the mono- and bilayer systems decreases upon the application of biaxial strain. Very interestingly, a semiconductor–metal transition was predicted for a tensile strain of about 8 % or a compressive strain of about 15 %. Authors of [12] realized a field-effect transistor with a single, two-dimensional layer of the MoS₂ as a conductive channel which demonstrated mobility, comparable to the achieved in thin silicon films or graphene nanoribbons. They claimed that such device could form the backbone of future electronics based on layered materials in which MoS₂ transistors could be fabricated on insulating boron nitride substrates. In the present work we analyze changes in electronic properties of MoS₂ starting from bulk material and ending by one-monolayer structure. Dispersion of phonon modes for bulk MoS₂ is considered as well.

Details of calculations

The structural optimizations and total energy calculations were performed with the help of the Vienna *ab initio* simulation package (VASP) [13] using density-functional theory (DFT) with projector-augmented wave (PAW)-type pseudopotentials both within generalized gradient approximation (GGA) of Perdew–Burke–Ernzerhof's (PBE) [14] and local density approximation

(LDA), as the latter method gave the lattice parameters closest to experimental data. In our calculations $4p$ semi-core states of Mo were treated as valence. Phonon dispersion curves were determined with the help of *Phonopy* package [15]. The total energy minimization was performed by calculation of Hellmann-Feynman forces and the stress tensor. The atomic relaxation was stopped when forces on atoms were less than 0.01 eV/\AA . The MoS_2 unit cell consists of 2 S-Mo-S monolayers (ML). To study the defect formation, the $1 \times 1 \times n_L$ and $2 \times 2 \times n_L$ cells (where n_L is the number of MLs) were used, while the number of MLs was considered from 1 to 4. The energy cutoff of 520 eV and $16 \times 16 \times 4$ and $6 \times 6 \times 3$ grids of Monkhorst-Pack points were used for calculations of bulk and layered material, respectively. We considered different width of vacuum and found that 15 \AA was quite enough to suppress the influence of neighboring layers. For the band structure plotting we have chosen up to 15 \mathbf{k} -points for each segment along the high-symmetry directions of hexagonal Brillouin zone.

Results

Some of the structures considered in our work are presented at fig. 1. The calculations show all the cases studied being stable. Resulting equilibrium structural parameters for bulk MoS_2 $a = 3.19 \text{ \AA}$ and $c = 13.15 \text{ \AA}$ (GGA) and $a = 3.12 \text{ \AA}$ and $c = 12.15 \text{ \AA}$ (LDA) were obtained, which are rather close to experimental values of $a = 3.16 \text{ \AA}$, $c = 12.29 \text{ \AA}$ [11]. Bulk MoS_2 was found to be an indirect-gap semiconductor with the E_g value of 1.2 eV (GGA) that is in good agreement with experimental gap of 1.23 eV [16] and 0.76 eV (LDA) (fig. 2). However, GGA simulation gave different from LDA results concerning the symmetry of the first transition: according to GGA, the transition occurs between the Γ (the valence band maximum, VBM) and the K (conduction band minimum, CBM) points, whereas LDA demonstrate the gap between the Γ point (VBM) and the point in Γ -K direction (CBM), like it was found in [17] and [18]. When the number of layers is larger than 2ML, a deviation in gap values in supercells becomes smaller and the bands dispersion and extrema location remains practically the same. The quite different situation, nevertheless, general for both approximations, occurs in the case of 1ML cell when VBM and CBM are situated in the K point, thus compound becomes direct gap semiconductor with the band gap of 1.85 eV (LDA) and 1.66 eV (GGA). Such behavior was experimentally observed by means of optical spectroscopy [8] giving the values of direct gap $\sim 1.8 \text{ eV}$ for monolayer MoS_2 and indirect gap of 1.29 eV for bulk material.

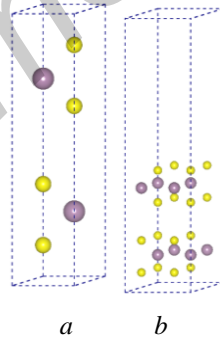


Fig. 1. MoS_2 unit cell (a) and $2 \times 2 \times 1$ supercell with vacuum (b); large balls – molybdenum atoms, small balls – sulfur atoms

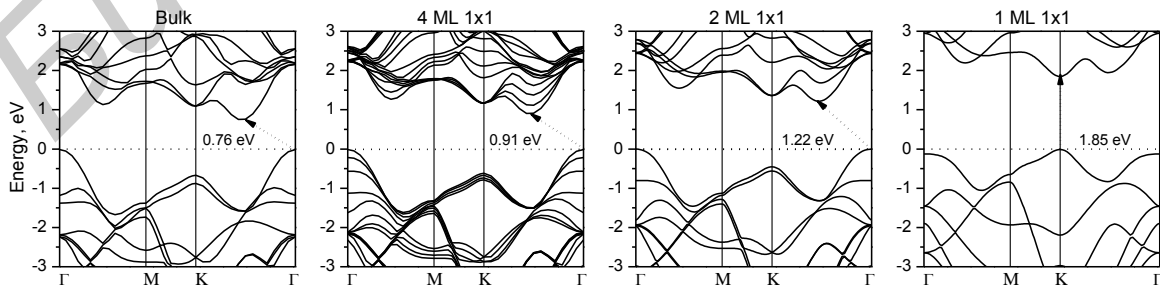


Fig. 2. The band structures of bulk and layered MoS_2 as calculated within LDA approximation

The correct description of the structural parameters is discussable, as the algorithms implemented in VASP completely neglect the van der Waals component of the interlayer interaction.

At the same time the LDA strongly overestimates the covalent part of the interlayer bonding and quite successfully reproduces the geometry and also gives reasonable results for layer phonon modes of different layered materials like graphene. We thus expect that LDA works reasonably well for the interlayer phonons of the MoS₂ [19].

In order to compare the obtained theoretical results with data of Raman spectroscopy [19] the vibrational properties of pure MoS₂ were analyzed. Phonon dispersion curves with the DOS (fig. 3) are found to be in good agreement with presented in [19] theoretical and experimental ones. This confirms that the interlayer interaction is described reasonably well within the used approach (even though it does not describe the proper physics of the interlayer forces). The dispersion phonon curves have three acoustic modes: two in-plane modes – vibrational longitudinal acoustic (LA) and transverse acoustic (TA), and one shear horizontal (ZA) mode, which is very similar to one of the graphene due to point-group symmetry [19].

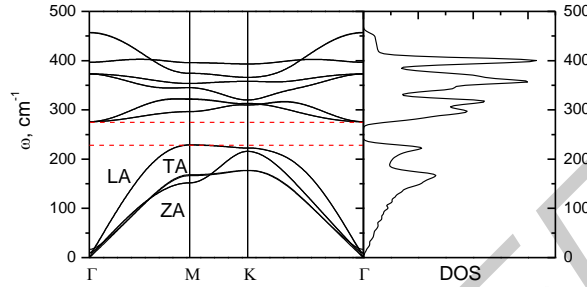


Fig. 3. Phonon dispersion curves and density of states of bulk MoS₂

In order to investigate the effect of sulfur vacancy in MoS₂ four different cases were considered: 1×1×2, 1×1×4, 2×2×2, 2×2×4. Fig. 4 represents the band structures of pure slabs with presented symmetry and the ones of the same slabs, but with one sulfur vacancy, what corresponds to 25, 12.5, 6.25 and 3.125 % vacancy concentrations, respectively.

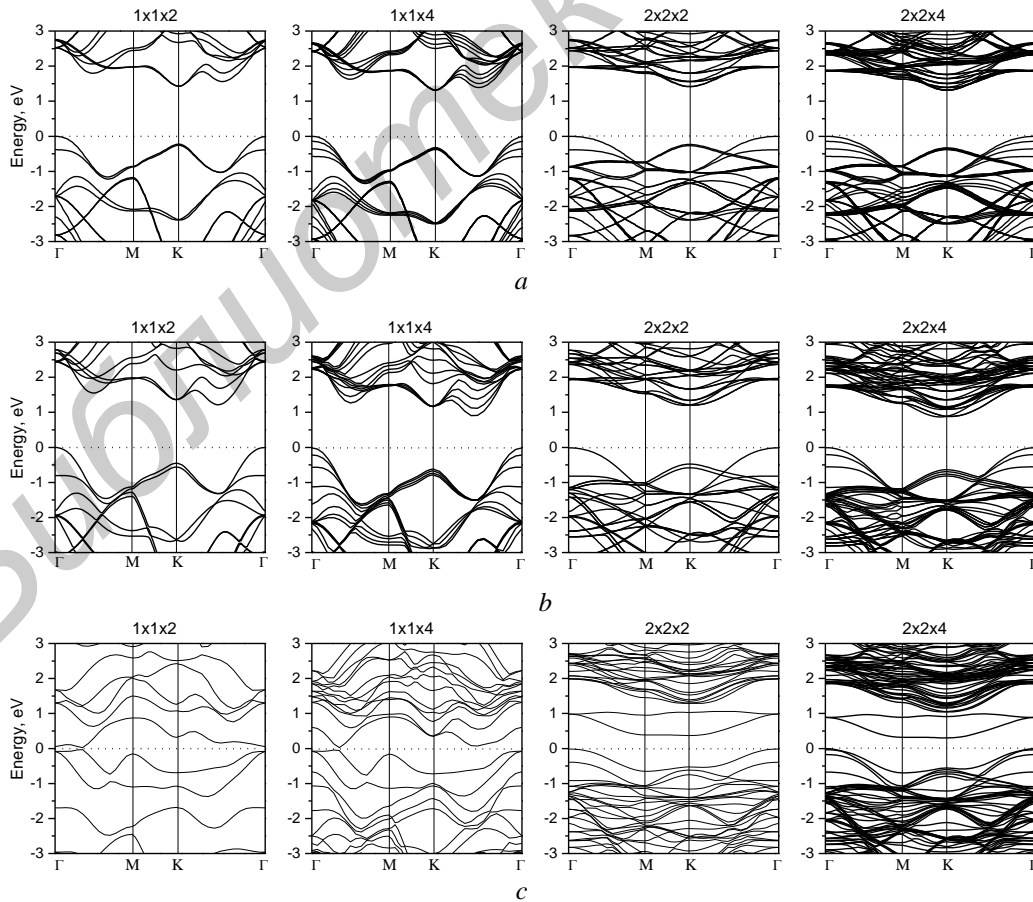


Fig. 4. The band structures of pure MoS₂ supercells, obtained within GGA (a) and LDA (b) approximations and with one S-vacancy in the middle (c) (LDA)

Upon studying the effect of sulfur vacancy in MoS₂ (fig. 4, *b*) it was found that when the sulfur atom was removed from the 1×1×*n_L* cell, it greatly affects the distance between atoms, so the changes occurred in the structure may be traced on band plots (fig. 4, *c*): large vacancy concentration leads to the gapless behavior with severe changes as compared to ideal band structure. Changes upon removing of sulfur atom from 2×2×*n_L* cell look not so drastically independent of whether atom was removed from the top or from the middle of the structure; in this case the vacancy located at the depth does not change the geometry of the slabs. New bands which sizably reduce the band gap appear in the forbidden gap, while the rest of the bands save practically the same dispersion except the upper valence band. The analysis of densities of states has shown that these bands are mainly formed by 4*d*-states of Mo atoms together with 3*p*-states of sulfur atoms, as it was already reported in [20]. An interesting feature is that these additional bands are formed by only neighboring to S vacancy atoms from the same layer.

Conclusion

Electronic and dynamical properties of molybdenum disulfide (MoS₂) were investigated by means of *ab initio* calculations. It was discovered that the decreasing of the slab width up to one monolayer increases the band gap and transforms indirect-gap semiconductor to a direct-gap one. Comparison of electronic properties of MoS₂ with sulfur vacancy in relation to pure MoS₂ has shown tendency to gapless behavior for small (1×1×2) supercells while large supercells (2×2×4) are characterized by the reduced band gap with some additional bands in the forbidden gap area. Thus, observed shrinkage of the energy gap upon vacancy introduction and transformations occurring upon decreasing the number of layers look perspective for band gap engineering. These characteristics and recent successful fabrication of transistors make MoS₂ a promising candidate for future device applications.

The work was done with the financial support of BRFFR-CNRS project № F13F-001 «Fundamental electronic and optical properties of two-dimensional crystals of refractory metal disulfides MoS₂, TiS₂, WS₂, and TaS₂ and associated compounds for nanoelectronic devices based on interference effects».

Literature

1. Geim A.K., Novoselov K.S. // Nature Materials. 2007. Vol. 6. P. 183–191.
2. Lalmi B., Oughaddou H., Enriquez H. et al. // Appl. Phys. Lett. 2010. Vol. 97. P. 22310 (1–4).
3. Feng B., Ding Z., Meng S. et al. // Nano Lett. 2012. Vol. 12. P. 3507–3511.
4. Jamgotchian H., Colignon Y., Hamzaoui N. et al. // J. Phys.: Condens. Matter. 2012. Vol. 24. P. 172001 (1–7).
5. Ayari A., Cobas E., Ogundadegbe O., Fuhrer M.S. // J. Appl. Phys. 2007. Vol. 101. P. 014507 (1–5).
6. Ho W., Yu J.C., Lin J. et al. // Langmuir. 2004. Vol. 20. P. 5865–5869.
7. Gmelin Handbook of Inorganic and Organometallic Chemistry. 8th ed. Vol. B7. Berlin, 1995.
8. Mak K.F., Lee C., Hone J. et al. // Phys. Rev. Lett. 2010. Vol. 105. P. 136805 (1–4).
9. Ramasubramaniam A., Naveh D., Towe E. // Phys. Rev. B. 2011. Vol. 84. P. 205325 (1–10).
10. Splendiani A., Sun L., Zhang Y. et al. // Nano Lett. 2010. Vol. 10. P. 1271–1275.
11. Scalise E., Houssa M., Pourtois G. et al. // Nano Res. 2012. Vol. 5. P. 43–48.
12. Radisavljevic B., Radenovic A., Brivio J. et al. // Nature Nanotech. 2011. Vol. 6. P. 147–150.
13. Kresse G., Furthmüller J. // Comput. Mater. Sci. 1996. Vol. 6. P. 15; Phys. Rev. B. 1996. Vol. 54. P. 11169–11186.
14. Perdew J.P., Burke K., Ernzerhof M. // Phys. Rev. Lett. 1996. Vol. 77. P. 3865–3838.
15. Togo A., Oba F., Tanaka I. // Phys. Rev. B. 2008. Vol. 78. P. 134106 (1–9).
16. Kam K.K., Parkinson B. // J. Chem. Phys. 1982. Vol. 86. P. 463–467.
17. Cheiwchanchamnangij T., Lambrecht W.R.L. // Phys. Rev. B. 2012. Vol. 85. P. 205302 (1–4).
18. Splendiani A., Sun L., Zhang Y. et al. // Nano Lett. 2010. Vol. 10. P. 1271–1275.
19. Molina-Sánchez A., Wirtz L. // Phys. Rev. B. 2011. Vol. 84. P. 155413 (1–8).
20. Kadantsev E.S., Hawrylak P. // Solid State Communications. 2012. Vol. 152. P. 909–913.